IJCSE International Journal of Computer Sciences and Engineering Open Access
Research Paper Volume-4, Issue-6 E-ISSN: 2347-2693

Enhancing Properties of Fiber Amplifier using Quantum Dots

Parnika De[1*] and Shailendra Singh[2]

[1*,2]*Department of Computer Engineering and Applications,*
National Institute of Technical Teachers Training and Research, India

www.ijcseonline.org

Received: May/22/2016 Revised: May/30/2016 Accepted: Jun/19s/2016 Published: Jun/30/ 2016

***Abstract*—** In recent years, semiconductor nanocrystals quantum dots (QDs) have been extensively studied because of their unique optical and electronic properties compared to their bulk counterparts. This ability to tune the bandgap of the QDs through the control of the particle size can provide near-infrared emission covering the important wavelength region for the fiber optic communication. We have doped the optical fiber core by quantum dots (QDs) to integrate the emission characteristics of quantum dots with propagation characteristics of optical fiber. In particular, narrow bandgap materials such as PbS and PbSe have attracted much attention. Due to the large bulk exciton Bohr radii of PbS (18 nm), quantum confinement effect can be achieved over the wide range of the particle size. Application specific QDs can be incorporated into the optical fiber core. It was reported that PbS nanoparticles could provide the emission over the whole transmission window (1200–1700 nm) of silica fibers, and therefore could be promising for all-wave optical amplifiers. We have carried out numerical investigation such amplifier characteristics and have shown incremental gain values. Simulation results show that it is possible to design an optical amplifier with flattened gain characteristics over S, C, and L bands with low noise figure, moderate optical signal to noise ratio and minimum gain of 10 dB.

***Keywords*—** Quantum dots; excitons; nanoparticles; quantum confinement; amplified stimulated emission

I. INTRODUCTION

Instant access to large amount of data has led to demands for large transmission capacity to carry the fast growing data traffic. As per the today and future requirements of transmission bandwidth and data rate, optical fibers promise enormous transmission bandwidths and high data rate H. Jong and L. Chao have reported the PbS QDs doped optical fiber amplifiers [1, 2]. The optical fiber wavelength range is divided in different regimes; the coarsest division is the 1.3 and 1.55 μm wavelength bands [3]. At 1.55 μm, a standard single mode fiber has the lowest attenuation of0.2 dB/km. The increase in data traffic, together with the advantages of fiber optics for data transmission; drive the development of optical components, especially those capable of all-optical processing without the need of complex opto-electro-optical conversion. Due to the losses of the optical fiber and the signal power differences in network nodes, amplification and regeneration of the optical signal are essential processes and the reason for the adoption of optical amplifiers in fiber communication.

- Rare earth-doped fiber or waveguide amplifiers

Gain band: Erbium (C, L-band), Thulium (S, U-band), Praseodymium (O-band) based on fluoride, telluride and silica materials

- Fiber Raman amplifiers

Gain band: 1.3 to 1.7 μm, tunable by the pump wavelength, if available realized as discrete or distributed pumped amplifiers

- Semiconductor optical amplifiers

Gain band: 1.2 to 1.7 μm, tunable by the InGaAsP composition based on InP substrates

Although erbium doped fiber amplifiers are available to amplify the optical signal in wavelength range of C and L bands, with very good gain and noise performance, and are widely employed in the optical network, the optical fiber amplifiers from S to L bands are yet to design in order to meet the growing demand of high speed and large bandwidth. Study shows that semiconductor nanocrystals quantum dots (QDs) have unique optical and electronic properties compared to their bulk counterparts. Quantum dots shows an important property to tune the bandgap through the control of the particle size can provide near-infrared emission covering the important wavelength region for the fiber optic communication. As the quantum dots' electron energy levels are discrete rather than continuous, the addition or subtraction of just a few atoms to the quantum dot has the effect of altering the boundaries of the bandgap. Changing the geometry of the surface of the quantum dot also changes the bandgap energy, owing again to the small size of the dot, and the effects of quantum confinement. Because the emission frequency of a dot is dependent on the bandgap, it is therefore possible to control

the output wavelength of a dot with extreme precision [4].In particular, narrow bandgap materials such as PbS and PbSe have attracted much attention. Due to the large bulk exciton Bohr radii of PbS (18 nm), quantum confinement effect can be achieved over the wide range of the particle size. PbS QDs could provide the emission over the whole transmission window (1200–1700 nm) of silica fibers, as a result optical amplifier with flattened gain characteristics over S, C, and L bands is possible to design.

For long-haul systems, the loss limitation has traditionally been overcome using optoelectronic repeaters in which the optical signal is first converted into an electric current and then regenerated using a transmitter. Such regenerators become quite complex and expensive for wavelength-division multiplexed (WDM) lightwave systems. An alternative approach to loss management makes use of optical amplifiers, which amplify the optical signaldirectly without requiring its conversion to the electric domain. Several kinds of optical amplifiers were developed to meet the system requirement, but they are limited to range of wavelengths. The best advantage of quantum dot doped fiber amplifier is tunable capability that means the operation wavelength depends on the size of quantum dot.
In order to achieve requirement of today and coming future of high channel capacity, it is very important to design an optical amplifier with flattened gain characteristics over S, C, and L bands. The objective of this project work is to study on a quantum dot doped fiber amplifier and their characteristics over S, C, and L bands. We aim to accomplish aforementioned amplification characteristics by changing the parameters of the quantum dot doped fiber amplifiers.

II. RELATED WORK

A quantum dot is a semiconductor whose excitons are confined in all three spatial dimensions. As a result, they have properties that are between those of bulk semiconductors and those of discrete molecules. They were discovered at the beginning of the 1980s by Alexei Ekimov in a glass matrix and by Louis E. Brus in colloidal solutions. The term "Quantum Dot" was coined by Mark Reed [4]. Quantum dots, also known as nanocrystals, are a special class of materials known as semiconductors, which are crystals composed of periodic groups of II-VI, III-V, or IV-VI materials. Semiconductors are a cornerstone of the modern electronics industry and make possible applications such as the Light Emitting Diode and personal computer. Semiconductors derive their great importance from the fact that their electrical conductivity can be greatly altered via an external stimulus (voltage, photon flux, etc), making semiconductors critical parts of many different kinds of electrical circuits and optical applications. Quantum dots are unique class of semiconductor because they are so small, ranging from 2-100 nanometers (10-500 atoms) in diameter. At these small sizes materials behave differently, giving quantum dots unprecedented tunability and enabling never before seen applications to science and technology [5].

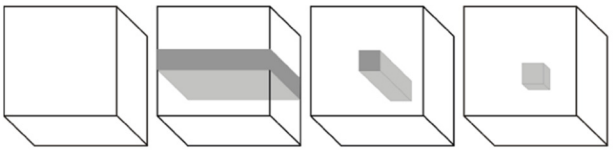

Fig. 1: Different semiconductor nanostructures: bulk-material, quantum-well, quantum-wire and quantum-dot [5].

If one is working with semiconductors it is important to clarify in which dimension they are existent. Semiconductors with quantum confinement in zero to three dimensions are shown in Fig. 1. The simplest form of a semiconductor is the bulk-semiconductor which is limited in no spatial direction and is therefore three-dimensional. If the extend is prevented in one dimension one gets a semiconductor-film, namely a quantum well. Decreasing the structure to one dimension one gets a semiconductor-line, a quantum-wire. The smallest existing nanostructure is the one used in this work, the zero-dimensional quantum dot whose extend is limited in all three dimensions.

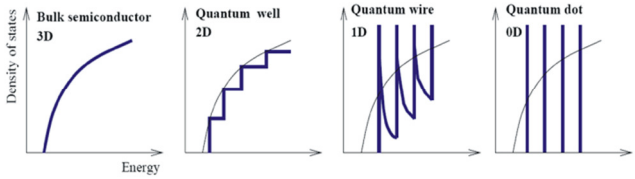

Fig. 2: Density of states for three, two, one and zero-dimensional systems [5].

The different nano-structures can be described through a so called confinement potential. Because of the restriction of the dimensions of extension there are energy edges between the single materials that build the potential. Thereby the movement of the carriers is restricted. This potential has influence on the density of states. In Fig. 2 the relation between the energy and the density of states is shown. A step-like density of states is given for a restriction in one dimension (quantum well). The density of states of the here relevant quantum dots has discrete energy-levels. Because of this characteristic, quantum dots are often referred to as artificial atoms [5].
For having a semiconductor emitting light one has to shift electrons from the valence-band to the conduction-band so that their subsequent recombination creates a photon. There are two possible ways of describing the new situation. First there is the two particle picture where the electron now situated in the conduction-band is the one particle and the

hole which it leaves in the valence band is considered as a second particle. The charge of the hole is the negative equivalent of the electron charge. This charge is essential to the implementation of the one particle picture, which is the second possibility to describe the excitation. Because of the charges and the Coulomb exchange interaction there is an attractive connection between the electron and the hole. For the purpose of simplification the electron-hole pair is considered as a quasiparticle which is named exciton. In Fig. 3 the potentials for both pictures are shown schematically. To assure the validity of the approximation made in this work with the introduction of the effective mass it has to be clarified that the excitons are considered to be Wannier-excitons. That is, the electron-hole pair, which represents the exciton, extends through the distance of some lattice constants. This definition is contrary to the so called Frenkel-excitons, where electron and hole a located within one lattice constant.

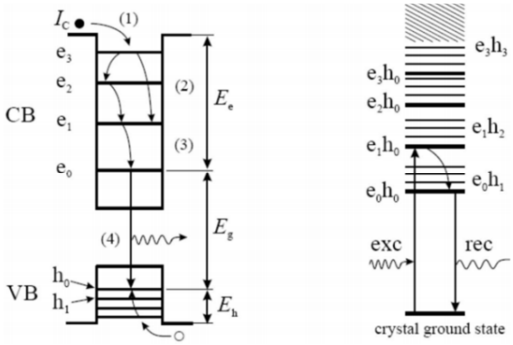

Fig. 3: Schematics of the two-particle-picture (electron and hole) on the left and of the one-particle picture (exciton) on the right. [8]

There are three major methods known to build up quantum dots:

1. Etching, where the dots are literally cut out of quantum wells.
2. Colloidal quantum dots that are created in liquids by chemical processes.
3. Self-assembling were the dots grow by themselves because of a sufficient mixture of different materials having suitable properties.

The latter is how the quantum dots used in this work are created. More concrete the dots where made by using molecular beam epitaxy (MBE), that is explained in the following. A schematic drawing of a MBE chamber is shown in Fig. 4. At first the material for application is evaporated in the effusion-chambers, which is in our case indium, arsenic and gallium. At second the molecular-beam is aligned to the substrate (GaAs). The atoms of the molecular beam settle on its surface. With the temperature of the substrate and the timing of applying material one can finally control the growth. Usually some layers of the substrate material are grown in advance of the nanostructures to overcome substrate irregularities. There are two kinds of phenomena corresponding to the self-organized growth of layers, layer- and island-growth. If the lattice constant of the substrate and the applied material are similar smooth layers are formed. Is there on the other hand a significant difference between the lattice constants strain is created which can prevent the growth of closed layers and lead to the appearance of islands [9].

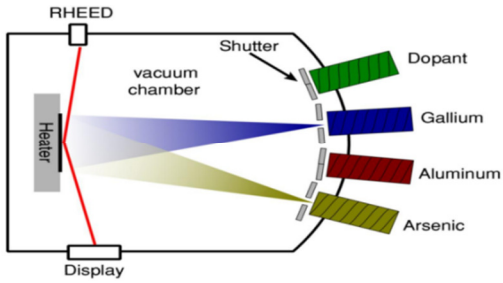

Fig. 4: Schematic presentation of a MBE-chamber which can be used to produce self-assembled quantum dots [9].

In most cases, which is true also for the current, first a closed coating of few mono-layers is formed which is called wetting layer. Only when the strain is big enough islands grow on top of it, see Fig. 5 a) top). In Fig. 5 b) an Atomic Force Microscopy (AFM) picture of an ensemble of such self-assembled quantum dots can be seen. Furthermore, chosen the right environmental conditions, i.e. giving the material not enough time to react to the stress, it is possible also to grow highly stressed quantum-wells [6].

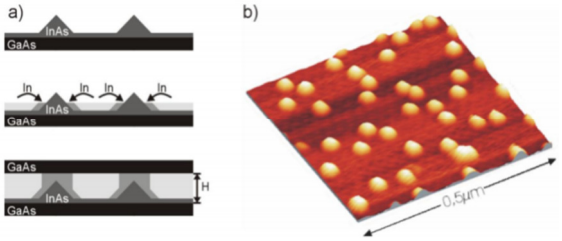

Fig. 5: a) Scheme of the growth of quantum dots. Top) Wetting layer with quantum dots. Middle) Application of a well meant to shift the emission wavelength. Bottom) Application of a spacer. b) AFM-picture of an ensemble of self-assembled quantum dots [6].

After creation of the quantum dots either a spacing layer is applied to the sample that acts as a barrier (mostly the substrate material is used) or, like in our case, a well is grown on top of the dots shifting the emission wavelength to more desired ones followed by the spacer (as can be seen in Fig. 5 a) middle). Such a nanostructure is called quantum dots in a well (DWELL). After that another layer of dots can be applied following the same methods. In our case 15 layers of quantum dots in a well where grown, the nominal density of the dots is n_{QD} $2x10^{10}$ cm^{-2} and the thickness of the spacer layer is 33-35 nm [9].

A. Quantum Confinement

The Quantum dots are also made out of semiconductor material. The main differences between the macrocrystalline semiconductor and the corresponding nanocrystalline material arise from two fundamental factors that are size related. The first one is associated to the large surface area to volume ratio of nanoparticles and the second one is related to the three-dimensional quantum confinement of their charge carriers. The electrons in quantum dots have a range of energies. The concepts of energy levels, bandgap, conduction band and valence band still apply. As we know exciton is a bound state of an electron and hole which are attracted to each other by the electrostatic Coulomb force. It is an electrically neutral quasiparticle that exists in insulators, semiconductors and some liquids. The exciton is regarded as an elementary excitation of condensed matter that can transport energy without transporting net electric charge. However, there is a major difference. Excitons have an average physical separation between the electron and hole, referred to as the Exciton Bohr Radius this physical distance is different for each material [10].

In bulk, the dimensions of the semiconductor crystal are much larger than the Exciton Bohr Radius, allowing the exciton to extend to its natural limit. However, if the size of a semiconductor crystal becomes small enough that it approaches the size of the material's Exciton Bohr Radius of the bulk semiconductor, α_B (typically in the 1 nm to 10 nm range which is still much larger than the semiconductor lattice constant, <1nm) then the electron energy levels can no longer be treated as continuous they must be treated as discrete, meaning that there is a small and finite separation between energy levels. This situation of discrete energy levels is called quantum confinement, and under these conditions, the semiconductor material ceases to resemble bulk, and instead can be called a quantum dot. This has large repercussions on the absorptive and emissive behavior of the semiconductor material [10].

A direct consequence of the 3D confinement is that the energy levels of the excited carriers (exciton) will become discrete and approach the molecular behavior as the particle size decreases. An ideal quantum dot can be treated like a spherical quantum box, and will display an atomic like absorption spectrum. The energies of the quantized states in the conduction and valence "band" can be calculated using the Schrödinger equation and the effective mass approximation [10].

In semiconductor materials, an electron can be excited across the band gap into the conduction band and leave a hole in the valence band simultaneously. By the attractive coulomb interaction, an excited electron in the conduction band and the resulting hole in the valance band may approach each other. Then, they form an electron-hole pair which is called an exciton. In case of the bulk PbS semiconductor, an electron-hole pair forms a weakly bound exciton in which an electron-hole separation distance is larger than the lattice constant of the crystal. The characteristic distance between these two charges can be expressed as [12]

$$\alpha_B^{ex} = \frac{h^2}{e^2}\epsilon\left[\frac{1}{m_e}+\frac{1}{m_h}\right] \quad (1)$$

- m_e and m_h - effective mass of electron and hole, respectively, e is the elementary charge
- ϵ - dielectric constant of the bulk semiconductor
- e - elementary charge

This distance is also known as the Bohr radius of the bulk exciton. When the size of this semiconductor is comparable to or smaller than the Bohr radius Eq. (1), the exciton will be confined spatially inside the semiconductor (dot). This results in quantum confinement, which gives a strong influence to the electronic and optical properties of the semiconductor. Based on the effective mass approximation, Brus [12, 13] showed for quantum dots that the energy gap between the lowest level of the conduction band (so called Lowest Unoccupied Molecular Orbital (LUMO)) and the highest level of the valence band (so called Highest Occupied Molecular Orbital (HOMO)) can be approximately calculated by

$$\Delta E \cong \frac{h^2\pi^2}{2R}\left[\frac{1}{m_e}+\frac{1}{m_h}\right]-\frac{1.8e^2}{\epsilon R} \quad (2)$$

where R is the radius of the quantum dot.

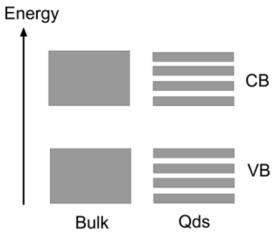

Fig. 6: A comparison of energy levels between a bulk semiconductor and a quantum dot.

In Eq. (2) the first term relates to the quantum localization which shifts the energy gap to higher energies as R^{-2}.The second term is the Coulomb term which shifts the energy to lower energies as R^{-1} . Consequently, the total energy gap (ΔE) increases in energy when decreasing the quantum dot diameter. Experimentally this effect can be observed as a blue shift of the absorption spectrum with decreasing quantum dot size. Moreover, quantum confinement causes that the valence band and the conduction band of the quantum dots consist of discrete energy levels, as shown in Fig. 6. These structures are often referred to as "artificial atoms". Changing the geometry of the surface of the quantum dot also changes the bandgap energy, owing again to the small size of the dot, and the effects of quantum confinement. Because the emission frequency of a dot is dependent on the bandgap, it is therefore possible to control

the output wavelength of a dot with extreme precision. The valence and conduction band in a bulk semiconductor consist of an energy continuum. On the contrary, the valence and conduction band in a quantum dot consist of discrete energy levels. The effective mass approximation model does not consider a number of important parameters, which are observed in real quantum dots, e.g., surface structure effects and size dependent structural lattice arrangements [13]. As a consequence, this model is not valid in predicting and explaining experimental results for very small quantum dots. To overcome these problems, more sophisticated models have been invented, such as the pseudopotential model by Krishna et al. [14].

III. METHODOLOGY

A two-level model is used to describe the energy-level, electron transition process, and is shown in Fig.1. The bandwidth [Eg(R)] of energy gap between valence and conductive bands are determined by following equation [17]:

$$(\alpha h\omega)^2 = (h\omega) - Eg(R) \quad (3)$$

Where

$$(Eg(R))^2 = (Eg)^2 + \left(\frac{2h^2 Eg}{m_*}\right)\left(\frac{\pi}{R}\right)^2 \quad (4)$$

and the energy gap depends on temperature (T) via following equation [17]:

$$E(T) = E_0 + \frac{\alpha T^2}{\beta + T} \quad (5)$$

Where

- E_g-phonon energy bandgap in single crystal,
- R -radius of QD,
- m_* -electron mass,
- h -Plank constant, respectively, and
- α and β are host-dependent parameters.

A laser at 0.800 µm is used to pump the doped waveguide, the up and low sublevels of the second level act as the excited and metastable levels

- W_{12pa}, W_{12pe}– represents the pump absorption and emission rates between the ground and the excited levels
- W_{12sa} , W_{12se} – represents the stimulated signal absorption and emission rates between the ground and the metastable levels
- A_{21} – represents the spontaneous emission rate from the metastable level to the ground level.
- N_1 , N_2 – are population densities of the ground level and the second level, respectively.

The behavior of the entire system can be represented through the absorption and emission cross sections shown in Fig. 8. The difference in spectral shape between the absorption and emission spectra is due to the thermal distribution of energy in conduction band and valence band of a quantum dots. The absorption and emission cross sections contain the exiton population distribution information.

There are some advantages of PbS QDs, such as PbS QDs have larger emission cross-section than Er^{+3} ions in addition to the large absorption cross-section. Furthermore, full width at half maximum (FWHM) intensity of photoluminescence from PbS QDs is approximately 190–250 nm, considerably larger than ~40 nm for 1.54 µm emission from $Er^{3+.}$ Such large FWHM was induced by the size dispersion of PbS QDs, which can also be tuned by the careful control of the heat-treatment. Therefore, it appears that PbS QDs provide promising features for the application to broadband fiber-optic amplifiers [18].

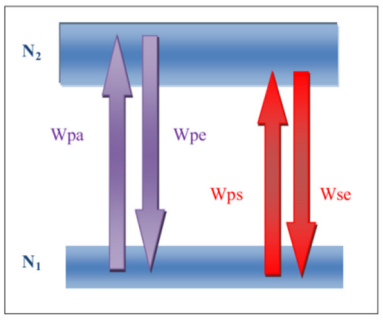

Fig. 7: Schematic of two-level system of QD-doped glass [17].

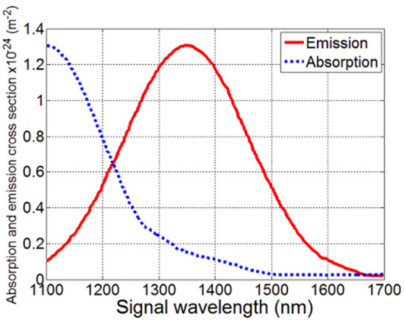

Fig. 8: Absorption and emission cross sections as functions of wavelength [17].

A. *Generalized Rate Equations without ASE*

From a two-level model of a quantum dot doped fiber amplifiers rate equations describing electronic transition without considering amplified stimulated emission (ASE) is given by [17]

$$\frac{\partial N_1}{\partial t} = -(W_{12pa} + W_{12sa})N_1 + A_{21}N_2 + (W_{21pe} + W_{21se})N_2 \quad (6)$$

$$\frac{\partial N_2}{\partial t} = \left(W_{12pa} + W_{12sa}\right)N_1 - A_{21}N_2 - (W_{21pe} + W_{21se})N_2 \quad (7)$$

$$N = N_1 + N_2 \quad (8)$$

Where
A_{21} is the radiative decay rate of the transition.
The radiative decay rate A_{21} is inversely proportional to the lifetime τ

$$A_{21} = \frac{1}{\tau} \quad (9)$$

We have

$$\frac{\partial N_1}{\partial t} = -\frac{\partial N_2}{\partial t} \quad (10)$$

At the steady state condition, we can consider:
$\frac{\partial N_1}{\partial t} = 0$ and $\frac{\partial N_2}{\partial t} = 0$

By solving above equation (6) and (7) for steady state condition, we get,

$$N_1 = \frac{(A_{21}+W_{12pe}+W_{12se})N}{W_{12pa}+W_{12sa}+A_{21}+W_{21pe}+W_{21se}} \quad (11)$$

$$N_2 = \frac{(W_{12pa}+W_{12sa})N}{W_{12pa}+W_{12sa}+A_{21}+W_{21pe}+W_{21se}} \quad (12)$$

The transition probabilities of pump and signal absorption and emission are given below in terms of respective cross-section values and respective powers:

$$W_{12sa} = \frac{\sigma_{sa}P_s}{h\nu_s A_{eff}}, W_{12se} = \frac{\sigma_{se}P_s}{h\nu_s A_{eff}}, W_{12pa} = \frac{\sigma_{pa}P_s}{h\nu_p A_{eff}}, W_{12pe} = \frac{\sigma_{pe}P_s}{h\nu_p A_{eff}} \quad (13)$$

- σ_{sa} and σ_{se}- represents the absorption and emission cross sections of the signal
- σ_{pa} and σ_{pe}- represents the absorption and emission cross sections of the pump

The power propagation equations describing pump and signal power propagating through the active fiber is given as [17],

$$\frac{\partial P_p(z,t)}{\partial z} = -P_p\Gamma_p\left(\sigma_{pa}N_1 - \sigma_{pe}N_2\right) - \alpha_p P_p \quad (14)$$

$$\frac{\partial P_s(z,t)}{\partial z} = -P_s\Gamma_s(\sigma_{se}N_2 - \sigma_{sa}N_1) - \alpha_s P_s \quad (15)$$

- Γ_s and Γ_p- represent the confinement factor
- α_p and α_s- denote the background loss of, signal and pump beams, respectively.

B. Amplified Spontaneous Emission

All the excited ions can spontaneously relax from the upper state to the ground state by emitting a photon that is uncorrelated with the signal photons. This spontaneously emitted photon can be amplified as it travels down the fiber and stimulates the emission of more photons from excited ions, photons that belong to the same mode of the electromagnetic field as the original spontaneous photon. This parasitic process, which can occur at any frequency within the fluorescence spectrum of the amplifier transitions, obviously reduces the gain from the amplifier. It robs photons that would otherwise participate in stimulated emission with the signal photons. It is usually referred to as ASE (amplified spontaneous emission). Ultimately, it limits the total amount of gain available from the amplifier.

To compute the ASE at the output of the fiber, we need to first calculate the spontaneous emission power at a given point in the fiber. This power is sometimes referred to as an equivalent noise power. For a single transverse mode fiber with two independent polarizations for a given mode at frequency ν_s, the noise power in a bandwidth $\Delta\nu$, corresponding to spontaneous emission, is equal to [19]

$$P_{ASE}^0 = 2h\nu_s\Delta\nu \quad (16)$$

The total ASE power at a point along the fiber is the sum of the ASE power from the previous sections of the fiber and the added local noise power P_{ASE}^0. This local noise power will stimulate the emission of photons from excited erbium ions, proportionally.
The propagation equation for the ASE power propagating in a given direction is

$$\frac{\partial P_{ASE(z,t)}}{\partial z} = -P_{ASE}\Gamma_s(\sigma_{se}N_2 - \sigma_{sa}N_1) + 2\sigma_{se}N_2\Gamma_s h\nu_s\Delta\nu - \alpha_s P_{ASE} \quad (17)$$

C. Generalized Rate Equations with ASE

As we see in section 3.2.2, amplified spontaneous emission is present in the system, which lowers the system performance. It is important to consider (amplified spontaneous emission rate equations are given by equation (3.16) and equation (3.17) as shown

$$\frac{\partial N_1}{\partial t} = -\left(W_{12pa} + W_{12sa} + W_{12ASE_a}\right)N_1 + A_{21}N_2 + (W_{21pe} + W_{21se} + W_{21ASE_e})N_2 \quad (18)$$

$$\frac{\partial N_2}{\partial t} = \left(W_{12pa} + W_{12sa} + W_{12ASE_a}\right)N_1 - A_{21}N_2 - (W_{21pe} + W_{21se} + W_{21ASE_e})N_2 \quad (19)$$

Similarly consider study state condition, we get,

$$N_1 = \frac{(A_{21}+W_{21pe}+W_{21se}+W_{21ASE_e})N}{W_{12pa}+W_{12sa}+W_{12ASE\_a}+A_{21}+W_{21pe}+W_{21se}+W_{21ASE\_e}} \quad (20)$$

$$N_2 = \frac{(W_{12pa}+W_{12sa}+W_{12ASE\_a})N}{W_{12pa}+W_{12sa}+W_{12ASE\_a}+A_{21}+W_{21pe}+W_{21se}+W_{21ASE\_e}} \quad (21)$$

And the power propagation equation describing pump, signal, and amplified spontaneous emission (ASE) power propagating through the active fiber is given equations (14), (15), and (17) as

$$\frac{\partial P_{p(z,t)}}{\partial z} = -P_p\Gamma_p(\sigma_{pa}N_1 - \sigma_{pe}N_2) - \alpha_p P_p \quad (22)$$

$$\frac{\partial P_{s(z,t)}}{\partial z} = P_s\Gamma_s(\sigma_{se}N_2 - \sigma_{sa}N_1) - \alpha_s P_s \quad (23)$$

$$\frac{\partial P_{ASE}(z,t)}{\partial z} = P_{ASE}\Gamma_s(\sigma_{se}N_2 - \sigma_{sa}N_1) + 2\sigma_{se}N_2\Gamma_s h\nu_s\Delta\nu - \alpha_s P_{ASE} \quad (24)$$

The transition probabilities of amplified spontaneous emission noise absorption and emission are given by

$$W_{12ASE\_a} = \frac{\sigma_{ASE\_a}P_{ASE}}{h\nu_{ASE}A_{eff}},\ W_{21ASE\_e} = \frac{\sigma_{ASE\_e}P_{ASE}}{h\nu_{ASE}A_{eff}} \quad (25)$$

Where σ_{ASE_a} and σ_{ASE_e} denote the absorption and emission cross sections of ASE, respectively. Generally, $\sigma_{ASE\_a} = \sigma_{sa}$ and $\sigma_{ASE\_a} = \sigma_{ASE\_e}$ In case of multiple signals used in system, the transition probabilities of pump, signal and amplified spontaneous emission noise absorption and emission are given by

$$W_{12sa} = \sum\frac{\sigma_{sa}P_s}{h\nu_s A_{eff}},\ W_{21se} = \sum\frac{\sigma_{se}P_s}{h\nu_s A_{eff}},\ W_{12pa} = \sum\frac{\sigma_{pa}P_p}{h\nu_p A_{eff}} \quad (26)$$

$$W_{21pe} = \sum\frac{\sigma_{pe}P_p}{h\nu_p A_{eff}},\ W_{12ASE\_a} = \sum\frac{\sigma_{ASE\_a}P_{ASE}}{h\nu_{ASE}A_{eff}},\ W_{21ASE\_e} = \sum\frac{\sigma_{ASE\_e}P_{ASE}}{h\nu_{ASE}A_{eff}} \quad (27)$$

D. Amplifier Noise and OSNR

Generally most of the amplifiers downgrade the SNR(signal to noise ratio) of the signals. The reason behind this is the spontaneous emission, which results in noise in the signal. The SNR degradation is measured by the parameter F_n. F_n is also called the amplifier noise figure. It is defined as

$$F_n = \frac{(SNR)_{in}}{(SNR)_{out}} \quad (28)$$

where SNR is the generated electric power when there is a conversion from optical signal to electric signal. F_n can vary depending on several parameters that is associated with thermal noise in the detector. F_n can simply be considered with shot noise only. If we consider an amplifier whose gain is G. Then we can write

$$P_{out} = GP_{in} \quad (29)$$

Therefore the SNR is given by

$$(SNR)_{in} = \frac{P_{in}}{2h\nu\Delta f} \quad (30)$$

where $< I > = RP_{in}$, the average photocurrent, R = q/h is the responsivity of a photodetector with unit quantum efficiency

$$\sigma_s^2 = 2qRP_{in}\Delta f \quad (31)$$

The amplifier noise figure is

$$F_n = \frac{(SNR)_{in}}{(SNR)_{out}} = \frac{1+2n_{sp}(G-1)}{G} \quad (32)$$

The parameter n_{sp} is the spontaneous-emission factor Along with the amplified signal, there is ASE power, which is given by the following equation [10]

$$P_{ASE} \approx 2n_{sp}(G-1)h\nu\Delta f \quad (33)$$

Then the amplifier noise figure can be given by

$$F_n = \frac{P_{ASE}}{h\nu\Delta f G} + \frac{1}{G} \quad (34)$$

We define the optical signal-to-noise ratio (OSNR) as the ratio of the output of the optical signal power to the ASE power which is shown by the following formula

$$OSNR = \frac{P_{out}}{P_{ASE}} = \frac{GP_{in}}{2n_{sp}(G-1)h\nu\Delta f} \quad (35)$$

IV. RESULTS

The emission spectrum as a function of wavelength is shown in Fig. 8; the emission spectrum covers the wavelength from 1100 to 1700 nm and centered around 1350 nm. The emission and absorption cross-section of pump beams of wavelength 800 nm are 0.8×10^{-24} m^{-2} and 3.4×10^{-24} m^{-2}, respectively. We have used conventional fiber with core radius a= 4 μm, optical fiber core refractive index, n = 1.59 with refractive index difference, Δ = 0.5%, loss coefficient, α= 0.3 dB/m, the bandwidth, Δυ = 125 GHz, and emission lifetime, τ = 240 μs. All the calculations and results are carried out at room temperature (RT).

The calculated noise figure and OSNR for QDs doped fiber amplifiers are shown in Fig. 9 and Fig 10. The minimum NF we have achieved is 3.3 dB. For the wavelengths (λ) 1100 nm – 1150 nm, NF is much high (> 10 dB). Noise figure value for S and C bands are lying between 3.3 dB – 6 dB, and for L band the NF value is varies from 6 dB to 8 dB. The maximum calculated value for OSNR is 14.5 dB, shown in Fig 10.

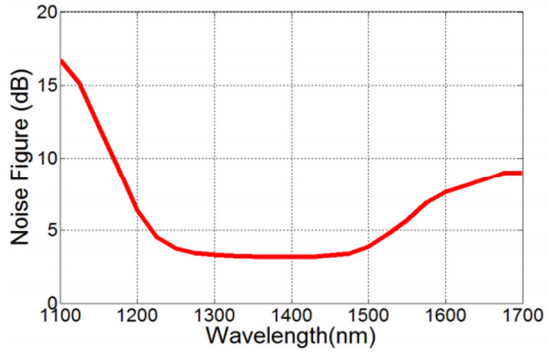

Fig 9: Noise figure variation of QDs doped fiber amplifiers (1100 nm – 1700 nm)

In the above diagram we can see that as the wavelength increases the noise figure decreases. This decreasing trend is followed till a certain limit after that limit the noise figure starts increasing which is not desirable. So the most preferable wavelength for the working of the quantum dots are between 1200nm to 1700nm approximately.

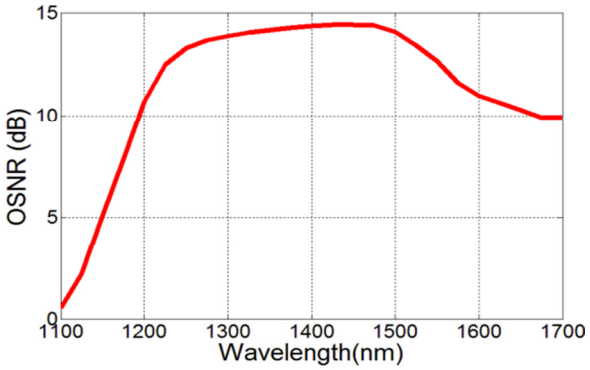

Fig 10: Variation of OSNR for QDs doped fiber amplifiers (1100 nm – 1700 nm)

In this diagram we will evaluate the results for OSNR (optical signal to noise ratio). Here we see that the OSNR increase after a certain bandwidth stay almost constant till a certain bandwidth and then starts decreasing. The trend followed in this diagram is same as the trend followed in the Fig 4.1. The OSNR stays maximum for the wavelength between 1200nm to 1700nm. So here through the graphs we have found out that the most suitable range of working of QD doped fiber amplifiers are between 1200nm to 1700nm.

V. CONCLUSION

Here we have reported a thorough study of quantum-dot fiber amplifiers, and has demonstrated that it has gain amplification capability for a large range of wavelengths, i.e. from 1200 nm to 1700 nm. The simulation is done using MATLAB and calculated the noise figure and OSNR value. Quantum dot doped fiber amplifiers have high value of loss coefficient, in the range of 0.3dB/m. So, the fiber length is an important parameter in the amplification of the signals, for the maximum amplification the fiber length needs to optimize. Simulation shows that it is possible to design and implement an optical amplifier with low noise figure, moderate optical signal to noise ratio.

System performance of optical amplifier is dependent on the gain characteristics of an amplifier. For satisfactory working of an amplifier, gain characteristics should be flattened.

REFERENCES

[1] W. Huang, Y.-Z. Chi, X. Wang, S.-F. Zhou, L. Wang, E. Wu, H.-P. Zeng, and J. R. Qiu, "Tunable infrared luminescence and optical amplification in PbS-doped glasses," *Chin. Phys. Lett.*, vol. 25, pp. 2518–2520, 2008.

[2] H. Jong and L.Chao, "Pbs quantum-dots in glassmatrix for universal fiber optic amplifier", *J. Mater. Sci: Mater. Electron.*, vol. 18, pp. S135–S139, 2007.

[3] G. P. Agrawal, "*Fiber-Optic Communication Systems,"* 3 ed. John Wiley & Sons, Inc., New York, 2002.

[4] http://en.wikipedia.org/wiki/Quantum_dot

[5] D. Bimberg, M. Grundmann, and N. N. Ledentsov, "*Quantum dot heterostructures,"* John Wiley, Chichester, 1999.

[6] S. M. Reimann and M. Manninen, "Electronic structure of quantum dots", *Rev. Mod. Phys.*, vol. 74, pp. 1283-1342, 2002.

[7] X. Michalet, F. F. Pinaud, L. A. Bentolila, J. M. Tsay, S. Doose, J. J. Li, G. Sundaresan, A. M. Wu, S. S. Gambhir, and S. Weiss, "Quantum dots for live cells, in vivo imaging and diagnostics," *Science,* vol. 307, pp. 538-544 (2005).

[8] Y. Masumoto and T. Takagahara, "*Semiconductor Quantum Dots*," Springer Verlag, Berlin, Heidelberg, New York, 2002.

[9] A. E. Zhukov, A. R. Kovsh, N. A. Maleev, S. S. Mikhrin, V. M. Ustinov, A. F. Tsatsul'nikov, M. V. Maximov, B. V. Volovik, D. A. Bedarev, Yu. M. Shernyakov, P. S. Kop'ev, Zh. I. Alferov, N. N. Ledentsov, and D. Bimberg, "Long wavelength lasing from multiply stacked InAs/InGaAs quantum dots on GaAs substrates," *Appl. Phys. Lett.*, vol. 75, pp. 1926-1934, 1999.

[10] C. R. Giles and D. Emmanuel, "Modeling erbium-doped fiber amplifiers," *J. Lightw. Technol.*, vol. 9, no. 2, pp. 271–283, 1991.

[11] T. Wang, F. Pang, K. Wang, R. Zhang and G. Liu, "Evanescent wave coupled semiconductor quantum dots fiber amplifier based on reverse Micelle method," Proceedings of the 7th IEEE, International Conference on Nanotechnology, Hong Kong, pp. 819–822, Aug. 2–5, 2007.

[12] Y. Wang, A. Suna, W. Mahler, R. Kasowski, "PbS in polymers. From molecules to bulk solids," J. Chem. Phys., vol. 87, pp. 7315-7322, 1987.

[13] L. E. Brus, "Electron-Electron and Electron-Hole Interaction in Small Semiconductor Crystallites: The Size Dependence of The Lowest Excited Electronic State," J. Chem. Phys., vol. 80, pp. 4403-4418, 1984.

[14] M. V. R. Krishna, and R. A. Friesner, "Quantum Confinement Effects inSemiconductor Clusters," J. Chem. Phys., vol. 95, pp. 8309-8321, 1991.

[15] F. W. Wise, "Lead salt quantum dots: The limit of strong quantum confinement," Acc. Chem. Res., vol. 33, no. 11, pp. 773–780, 2000.

[16] K. Nakagawa, S. Nishi, K. Aida, and E. Y oneda, "Trunk and distribution network application of Erbium-doped fiber amplifier," J. Lightwave Technol.,vol.9, pp. 198-221, 1991.

[17] C. Jiang, "Ultrabroadband Gain Characteristics of a Quantum-Dot-Doped Fiber Amplifier," IEEE J. Sel. Top. Quantum Electron., Vol. 15(1), pp. 140–144, 2009.

[18] L. Chao, H. Jong, Z. Xianghua, and A. Jean-Luc, "Photoluminescence of PbS quantum dots embedded in glasses," J. Non-Cryst. Solids, vol. 354, pp. 618–623, 2008.

[19] F. C. BECKER, N. A. OLSSON, J. R. SIMPSON, "Erbium-Doped Fiber Amplifiers Fundamentals and Technology," Optics and Photonics, New York, 1997.

[20] C. R. Giles and D. Emmanuel, "Modeling erbium-doped fiber amplifiers," J. Lightw. Technol., vol. 9, no. 2, pp. 271–283, 1991.

[21] K. Thyagarajan, Jagneet Kaur, "A novel design of an intrinsically gain flattened erbium doped fiber," Optics Communications, vol. 183. pp. 407–413, 2000.

[22] Cheng Cheng, "A Multiquantum-Dot-Doped Fiber Amplifier with Characteristics of Broadband, Flat Gain, and Low Noise," J. of Lightw . Technol., vol. 26, no. 11, pp. 1404-1410, 2008.

AUTHOR'S PROFILE

Parnika De: Doing MTech. In Computer Science from National Institute of Technical Teachers Training and Research. Research area future network technologies and machine learning.

Shailendra Singh: Professor and Head in the Department of Computer Engineering and Applications. Key research areas are machine learning and cyber security.